Cerebral Cortex July 2005;15:913-920
doi:10.1093/cercor/bhh190
Advance Access publication September 30, 2004

Basal Ganglia and Cerebellar Inputs to 'AIP'

Dottie M. Clower[1], Richard P. Dum[1] and Peter L. Strick[1,2,3]

[1]Pittsburgh Veterans Affairs Medical Center, University of Pittsburgh School of Medicine, Pittsburgh, PA, USA, [2]Center for the Neural Basis of Cognition, University of Pittsburgh School of Medicine, Pittsburgh, PA, USA and [3]Departments of Neurobiology, Neurosurgery and Psychiatry, University of Pittsburgh School of Medicine, Pittsburgh, PA, USA

The anterior intraparietal area (AIP) is a subregion of area 7b in posterior parietal cortex. AIP neurons respond to the sight of objects, as well as to the act of grasping them. We used retrograde transneuronal transport of rabies virus to examine subcortical inputs to AIP in the monkey. Virus transport labeled substantial numbers of neurons in the substantia nigra pars reticulata (SNpr), as well as in the dentate nucleus of the cerebellum. The hotspots of labeled neurons in SNpr and in dentate after AIP injections were separate from those created by virus injections into several other parietal or frontal regions. These observations provide the first evidence that a major output nucleus of the basal ganglia, the SNpr, projects to a region of posterior parietal cortex. In addition, our findings provide further support for the concept that posterior parietal cortex is a target of cerebellar output.

Keywords: basal ganglia, cerebellum, dentate nucleus, posterior parietal cortex, rabies virus, substantia nigra, transneuronal tracing

Introduction

Physiological and anatomical studies in monkeys have identified a unique subregion of area 7b within inferior parietal cortex termed the anterior intraparietal area (AIP). AIP neurons either have visual responses to the three-dimensional features of objects, motor responses to object manipulation or the combination of the two types of responses (Godschalk and Lemon, 1989; Taira *et al.*, 1990; Sakata and Taira, 1994; Sakata *et al.*, 1995, 1998; Murata *et al.*, 1996, 2000). AIP can be defined anatomically based on its extensive interconnections with the ventral premotor area (PMv or area F5) (Chavis and Pandya, 1976; Petrides and Pandya, 1984; Godschalk *et al.*, 1984; Matelli *et al.*, 1984, 1986; Neal *et al.*, 1990; Ghosh and Gattera, 1995; Luppino *et al.*, 1999; Tanne-Gariepy *et al.*, 2002; see also Preuss and Goldman-Rakic, 1991; Lewis and Van Essen, 2000). Indeed, neurons in the PMv display visuomotor responses that are in many respects similar to those of AIP neurons. However, AIP contains more neurons that are exclusively responsive to the visual features of an object, whereas PMv contains more neurons that are selectively responsive during movement (Murata *et al.*, 1997, 2000). Thus, AIP and PMv are thought to be nodes in a cortical network concerned with processing the visual features of objects to specify the appropriate grasping patterns for manipulating them (Sakata *et al.*, 1997; Oztop and Arbib, 2002).

With the exception of some cortical interconnections, the anatomical inputs to AIP have not been well characterized. In recent studies we have shown that an adjacent portion of area 7 is the target of output from the dentate nucleus of the cerebellum while other portions of area 7 receive input from either the superior colliculus or CA1 of the hippocampus (Clower *et al.*, 2001a). We wondered whether one or all of these subcortical systems were a source of input to AIP. For example, perhaps some of the 'visual' properties of AIP neurons are the result of input from the superior colliculus. Similarly, some of the 'motor' properties of AIP neurons could be a consequence of input from the cerebellum. In addition, given the extensive interconnections between AIP and PMv, we sought to examine whether these two cortical areas received inputs from common sources. PMv is the target of output from both the dentate and the internal segment of the globus pallidus (GPi) (Hoover and Strick, 1993; Dum and Strick, 2002). While there is no prior evidence for basal ganglia input to regions of posterior parietal cortex, some basal ganglia disorders result in symptoms that closely mimic parietal lobe dysfunction (Danta and Hilton, 1975; Boller *et al.*, 1984; Richards *et al.*, 1993; Hocherman and Giladi, 1998; Barrett *et al.*, 2001; Lee *et al.*, 2001a,b; Montse *et al.*, 2001). These observations raise the possibility that regions of posterior parietal cortex might also be targets of output from the basal ganglia.

To examine these issues, we used retrograde transneuronal transport of rabies virus after localized injections into AIP. The parameters for using rabies as a transneuronal tracer have been examined extensively in the cebus monkey (e.g. Kelly and Strick, 2000, 2003). In addition, we have examined the subcortical inputs to a number of cortical regions in the cebus monkey, including areas of posterior parietal, motor, prefrontal and inferotemporal cortex (Hoover and Strick, 1993, 1999; Lynch *et al.*, 1994; Middleton and Strick, 1996, 1997, 2001; Clower *et al.*, 2001a,b; Middleton and Strick, 2001; Dum and Strick, 2003). To be able to use all of this prior data for comparison, we chose to perform this experiment in the same species. However, prior anatomical and physiological experiments on AIP have been performed in macaques. Because AIP can be defined based on its interconnections with PMv, we used this anatomical feature to identify the location of AIP in the cebus monkey. We then injected the cebus AIP with rabies virus to define its subcortical inputs.

Our results show that AIP is the target of both basal ganglia and cerebellar output. Approximately equivalent numbers of neurons from each subcortical system project to AIP. In addition, the number of basal ganglia and cerebellar neurons that project to AIP is comparable to the number that project to individual areas of premotor and prefrontal cortex. Furthermore, the origins of the densest subcortical inputs to AIP are largely separate from the origins of the densest input to PMv. Abstracts of some of these results have been reported elsewhere (Clower *et al.*, 2001b, 2002).

Materials and Methods

The procedures adopted for this study and the care provided experimental animals conformed to the regulations detailed in the National

Institutes of Health Guide for the Care and Use of Laboratory Animals. All protocols were reviewed and approved by the Institutional Animal Care and Use Committees. The biosafety precautions taken during rabies virus tracer experiments conformed to or exceeded Biosafety Level 2 (BSL-2) regulations detailed in Biosafety in Microbiological and Biomedical Laboratories (Health and Human Services Publication 93-8395). A detailed description of the procedures for handling virus and virus-infected animals is presented in Kelly and Strick (2000); see also Strick and Card (1992) and Hoover and Strick (1999).

To conduct these experiments it was necessary to identify the location of AIP in the cebus monkey. In macaques, AIP is the region of posterior parietal cortex that is most densely connected with the PMv. We used this connection to define AIP in the cebus monkey. In two monkeys we located the region of area 7 that contained large numbers of labeled neurons after an injection of a conventional tracer into the digit representation of the PMv.

In three monkeys we injected AIP with rabies virus to label basal ganglia and cerebellar neurons that project (via the thalamus) to this cortical area. Finally, in an additional animal, we injected the AIP with conventional tracers to identify the source of its thalamic input.

Conventional Tracer Experiments

Surgical Procedures

Our methods for intracortical stimulation and tracer injections have been described fully in prior publications (Strick and Preston, 1982a,b; Holsapple *et al.*, 1991; Hoover and Strick, 1999). Briefly, all surgical procedures were performed under aseptic conditions. Once the animal was anesthetized with Telazol, it was placed in a stereotaxic frame and an appliance was secured to its skull with small screws and dental acrylic. The appliance served as an atraumatic anchor to hold the animal's head during the stimulation phase of the experiment. A large craniotomy was performed over the appropriate cortical area and the dura was opened. The cortical surface was protected from desiccation with warm surgical grade silicone.

Physiological Mapping

We used parylene coated Elgiloy microelectrodes (Suzuki and Azuma, 1976; impedance = 0.6–1.4 MΩ @ 1 kHz) to deliver intracortical stimuli. Cathodal pulses (12–32 pulses, 0.2 ms duration, 333 Hz, 1–50 μA) from a constant current stimulator were delivered at a standard depth of 1500 μm. The motor response evoked by intracortical stimulation was determined by visual observation and muscle palpation. The response at each site was defined as the movement or muscle contraction that was evoked at threshold- the stimulus intensity at which the response occurred on 50% of the trials. The results of physiological mapping were entered into a custom designed computer database for on-line acquisition and analysis of data from mapping experiments.

Tracer Injections

After we identified the digit representations in the PMv, we used a Hamilton syringe with a 28 gauge fixed needle to inject diamidino yellow (DY, 2% in distilled water, 0.4 μl per injection) into the PMv of one animal (R15) and fast blue (FB, 5% in distilled water, 0.3 μl per injection) into the PMv of the other (R24). Penetrations were spaced ~1 mm apart except to avoid blood vessels. The tracers were injected at a depth of 1.5 mm below the cortical surface. The needle was allowed to remain in place for 3 min after each injection. When the injections were completed, the exposed cortical surface was covered with dura and silastic, and the wound closed in anatomical layers. After a 12 day survival period, each animal was tranquilized (ketamine, 25 mg/kg, i.m.), deeply anesthetized (Nembutal, 36 mg/kg, i.p.) and perfused transcardially using a multi-stage procedure (Rosene and Mesulam, 1978; Mesulam, 1982).

Tissue Processing

Following the perfusion, the brain was blocked and stored at 4°C with 20% glycerin added as a cryoprotective agent for 4–7 days (Rosene *et al.*, 1986). Blocks of brain were frozen (Rosene *et al.*, 1986) and serially sectioned in the coronal plane at a thickness of 50 μm. Every tenth section was counterstained with cresyl violet for cytoarchitectonic analysis (Mesulam, 1982).

Analytic Procedures

Every fourth to eighth section was examined for DY and FB labeled neurons using a light microscope and epifluorescence illumination (Leitz filter D). Injection sites, section outlines and labeled cells were plotted using a computer-based charting system (MD2, Minnesota Datametrics). This system uses optical encoders to sense *X–Y* movements of the microscope stage and stores the coordinates of charted structures (e.g. section outlines, injection site zones and labeled neurons). The extent of the injection site was compared with the location of the identified digit representation by superimposing the outline of the reconstructed injection site over the map of movements evoked at each penetration site. Maps of individual sections through parietal cortex were aligned interactively on the computer. Sections were unfolded and used to construct 2-D maps of the cortex that indicated the location of labeled neurons in relation to morphological features (Dum and Strick, 1991; He *et al.*, 1993, 1995).

Conventional Tracer Injection into AIP

Six injections of DY (2% in distilled water, 0.4 μl per injection) were placed in AIP. The injections were made ~1.5 mm apart at a depth of 1.5 mm. Sections were plotted every 200 μm through the thalamus. All other procedures were as described above.

Virus Tracer Experiments

Virus Injections

We injected rabies virus into the AIP region of parietal cortex of three monkeys (Cebus apella). The method for rabies virus surgery has been described previously (Kelly and Strick, 2000). Briefly, the animals were anesthetized with isoflurane, and a craniotomy was performed over the parietal lobe. The dura was incised and reflected to expose the cortex. We used a 5 μl Hamilton syringe with a 28–32 gauge removable needle to place multiple injections (0.2 μl per site) of virus into the targeted region. Injections were spaced 0.5–1.0 mm apart except to avoid blood vessels. Ninety injections were made in each animal (three injection depths at 30 injection sites). Following each injection into the cortex, the needle was left in place for 2 min. Surgery was completed as described above. Following the surgery, animals were placed in a BSL-2 isolation room for further observation and recovery. All animals received dexamethasone (0.1–0.5 mg/kg, i.m. or p.o.) and buprenorphine (Buprenex®, 0.01 mg/kg, i.m.). After a survival period of 3–4 days, the animals were perfused as described previously.

Tissue Processing

Brain tissue was processed as described in the previous section. To identify neurons labeled by virus transport, we processed free-floating tissue sections according to the avidin-biotin-peroxidase method (ABC®; Vectastain, Vector Laboratories, Inc., Burlingame, CA) using antibodies directed against rabies virus (Kelly and Strick, 2000). At least every other section from these animals was reacted. Sections were mounted onto gelatin-coated glass slides, air dried, and then coverslipped with either Artmount® or DPX®.

Analytic Procedures

Approximately every other section was examined for labeled neurons under bright-field, dark-field, and polarized illumination. Sections through the injection sites, frontal lobe, GPi, SNpr and dentate nucleus were plotted using a computerized charting system (MD2, Minnesota Datametrics, Inc., St. Paul, MN).

Results

Location of AIP in the Cebus Monkey

AIP is the region of posterior parietal cortex that is most densely interconnected with the PMv (Luppino *et al.*, 1999; Tanne-Gariepy *et al.*, 2002). Therefore, to identify AIP in the cebus monkey we examined the origin of parietal lobe projections to the hand representation of the PMv in two animals. We used intracortical stimulation to define the hand representation in each animal prior to the tracer injections (Fig. 1*A*). We then

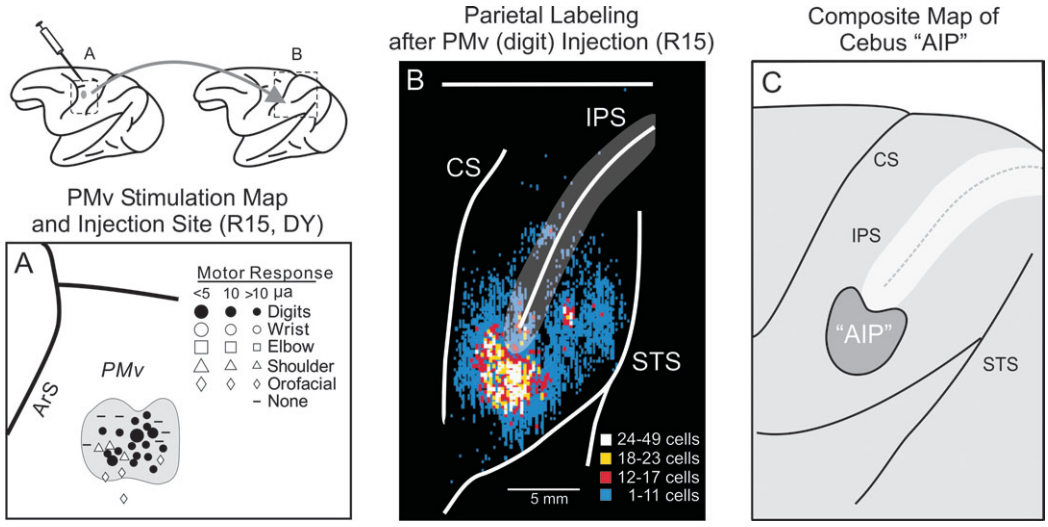

Figure 1. Localization of AIP in the cebus monkey based on corticocortical connectivity with PMv. (*A*) Map of microstimulation sites (symbols) on the cortical surface of cebus monkey R15 and boundary of the digit region of PMv injected with diamidino yellow (DY). (*B*) Cortical surface map showing density and location of labeled neurons after DY injection at the site shown in (*A*). (*C*) Composite map indicating the region within parietal cortex where densest labeling occurred after injection of the digit representation in PMv in experiments R15 and R24 (shaded area). AIP, anterior intraparietal area; ArS, arcuate sulcus; CS, central sulcus; IPS, intraparietal sulcus; PMv, ventral premotor area; STS, superior temporal sulcus.

injected the hand area with a fluorescent tracer. In animal R15 we injected DY and in animal R24 we injected FB.

In both animals we found large numbers of labeled neurons on the cortical surface just lateral to the tip of the intraparietal sulcus (Fig. 1*B*,*C*). The regions of dense labeling in the two animals overlapped considerably. The labeled region extended rostral to the tip of the intraparietal sulcus in R15 and caudal to the tip of the sulcus in R24. We operationally defined AIP as the region where dense labeling was present in both animals (Fig. 1*C*, 'AIP'). All of our virus injection sites were aimed at this region. Note that AIP in the cebus monkey is somewhat lateral and rostral to the location of AIP in the macaque (Godschalk *et al.*, 1984; Matelli *et al.*, 1984, 1986; Taira *et al.*, 1990; Ghosh and Gattera, 1995; Murata *et al.*, 2000; Tanne-Gariepy *et al.*, 2002).

Subcortical Input to AIP

We injected AIP with rabies virus (CVS-11) in three cebus monkeys (Fig. 2*B*). We set the survival time (3–4 days) to allow retrograde transport of virus from the injection site to first-order neurons in the thalamus and then, retrograde trans-neuronal transport of virus from these first-order neurons to second-order neurons in subcortical sites. Maps of labeled neurons in the frontal lobe showed that large numbers of labeled neurons overlapped the hand representation of the PMv in each animal (e.g. Fig. 2*A*). This observation confirmed that the injection sites were accurately placed within AIP.

We scanned every fifth section through basal ganglia, cerebellum, hippocampus and superior colliculus for second-order neurons labeled by transneuronal transport of virus. Substantial numbers of labeled neurons were found only at two sites: the substantia nigra (mean = 297, range = 180–490) and the dentate nucleus (mean = 283, range = 152–526) (Figs 3 and 4, Tables 1 and 2). A small number of labeled neurons also were consistently found in GPi (mean = 45, range = 24–64). A moderate number of labeled neurons (n = 94) were present in the posterior interpositus in only one (AIP_2) of the three animals.

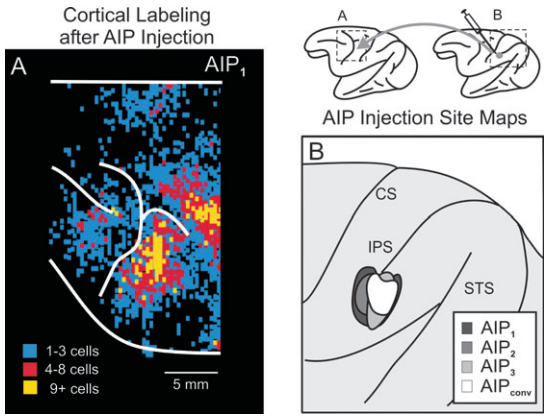

Figure 2. Localization of injection sites in AIP of the cebus monkey. (*A*) Cortical surface map showing the density and location of labeled neurons in the hand region of PMv after injections of rabies in AIP_1. (*B*) Composite map of AIP injection sites for three rabies experiments (AIP_1–AIP_3) and one conventional tracer (DY) experiment (AIP_{conv}).

In total, the number of labeled neurons in the output nuclei of the cerebellum and basal ganglia varied from animal to animal by a factor of ~3 (Table 1). However, the ratio of cerebellar to basal ganglia output neurons was nearly 1:1 in all three animals. Thus, AIP is the target of output from both the cerebellum and the basal ganglia, and the magnitude of this output is comparable from the two sources.

In the substantia nigra, labeled neurons were broadly distributed in the caudal two-thirds of the nucleus within the pars reticulata (SNpr) (Fig. 3). Although the absolute number of neurons labeled in the nigra varied from animal to animal (Table 1), the rostro-caudal distribution of labeled neurons was relatively consistent (Fig. 3, top). At rostral levels of the nigra, second-order neurons tended to be located in the dorsal portion of the nucleus. The distribution of labeled neurons shifted to a more ventral location at more caudal levels of the nucleus. Some authors have further subdivided the nigra into a pars reticulata region where cells uniformly do not stain with

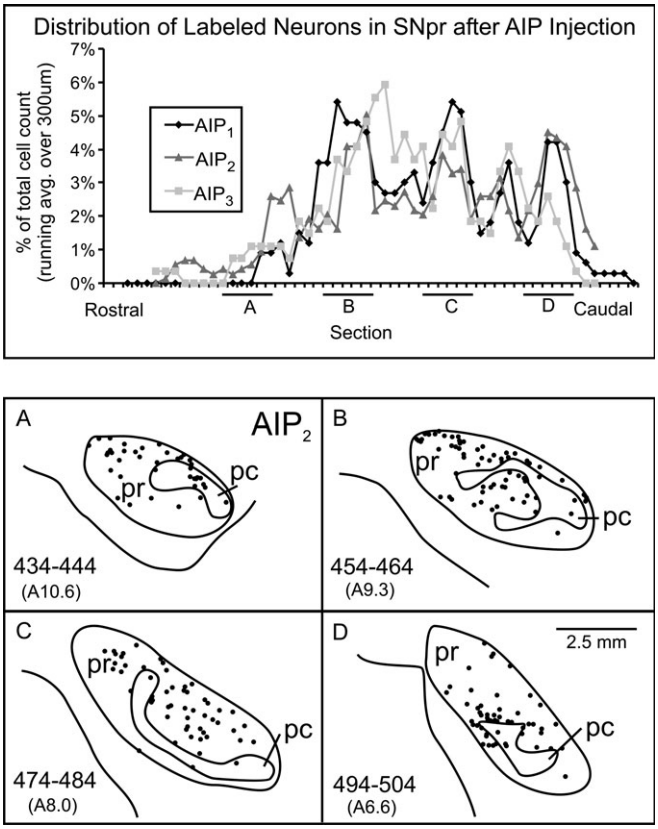

Figure 3. Distribution and density of SNpr neurons that project to AIP. Top: rostrocaudal distribution of labeled neurons in SNpr after AIP injections of rabies in three experiments (AIP_1–AIP_3). Bottom: cross sections of the substantia nigra showing the location of 'second-order' neurons (dots) labeled after transport of rabies virus injected in AIP. Each panel includes the labeled neurons from five sections (100 μm apart). Numbers in parentheses below section numbers indicate approximate rostrocaudal position of the sections according to Olszewski (1952). SNpc; substantia nigra pars compacta; SNpr, substantia nigra pars reticulata.

tyrosine hydroxylase (TH-negative) and a pars mixta region where TH-negative and TH-positive cells are intermingled (Francois *et al.*, 1984; Langer and Graybiel, 1989; Williams and Goldman-Rakic, 1998). The nigra neurons labeled after virus injections into AIP were found in both of these regions.

In the dentate nucleus, labeled neurons were widely distributed in the caudal two-thirds of the nucleus (Fig. 4). In all three of our experimental animals the densest site of labeled neurons after AIP injections was located dorsally at mid rostro-caudal levels of the dentate (Fig. 4, top-left, top-middle, *A*,*B*). A second small patch of dense labeling was present in two of the three animals (AIP_2 & AIP_3) in the caudal third of the dentate (Fig. 4, top-left, top-middle, *C*). These labeled neurons were located at a site we have previously shown to be near the origin of output to an adjacent portion of area 7b (Fig. 4, top-right; Clower *et al.*, 2001a,b; Dum *et al.*, 2002; Dum and Strick, 2003). A third, very small patch of labeled neurons was present in two of the three animals (AIP_2 & AIP_3) in the most ventral and medial part of the dentate (Fig. 4, top-left, top-middle, *B*). Finally, a low-density field of labeled neurons was present between the dorsal AIP site and the more caudal and ventral area 7b site (Fig. 4, top-left and top-right). Scattered labeled neurons were found in this region in all the animals that received virus injections into AIP. The lightly shaded ellipse in Fig. 4 (top-right) indicates an approximation of the limits of this field. Despite its low density, the field contained between two-thirds and three-quarters of the total cells that project from the dentate (via the thalamus) to AIP. It is notable that the field overlaps the region of the dentate that we have previously shown to be the origin of projections to M1 and the PMv (Fig. 4, top-right; Dum *et al.*, 2002; Dum and Strick, 2003).

'Direct' Subcortical Input AIP

In one cebus monkey we used a conventional tracer to: (i) identify thalamic nuclei that might mediate the retrograde transneuronal transport from AIP to the cerebellum and basal ganglia and (ii) confirm that no cerebellar or basal ganglia neurons project directly to AIP. Injections of DY into AIP (Fig. 2*B*, AIP_{conv}) resulted in focal accumulations of labeled neurons in multiple thalamic nuclei including the medial and lateral pulvinar, the oral pulvinar, LP, CnMd, VPLc, VPLo, VLc, CL, MDmf, VPI, VLm and PCn (not illustrated). Regions in several of these thalamic nuclei (e.g. VLc, MDmf, CL) are known to be the site of termination of cerebellar or nigral efferents (for references and review, see Percheron *et al.*, 1996). Thus, the dentate and nigral labeling we observed after virus injections could be mediated by retrograde transneuronal transport via these regions of the thalamus.

DY injections into AIP labeled a small number of neurons in A9 near the dorsal border of SNpr. However, no labeled neurons were seen in the core of SNpr, GPi or in any of the deep cerebellar nuclei following these injections. Thus, all of the labeled neurons we found in the basal ganglia and cerebellum following AIP injections of virus were second-order neurons labeled by retrograde transneuronal transport via the thalamus.

Discussion

Virus tracing has enabled us to demonstrate that AIP is the target of both cerebellar and basal ganglia output. Indeed, the number of basal ganglia and cerebellar neurons that project to AIP is comparable to the number that project to individual areas of motor and prefrontal cortex (Table 2). Thus, a considerable component of basal ganglia and cerebellar output is devoted to influencing the functional operations of posterior parietal cortex. In a prior study we examined subcortical inputs to other portions of area 7. We found that area 7a is the target of output from CA1 in the hippocampus, that the lateral intraparietal area (LIP) is the target of output from the superior colliculus and that a sulcal region of area 7b is the target of cerebellar output (Clower *et al.*, 2001a,b). These results, together with those from the present study, indicate that there is a complex topography to the pattern of subcortical inputs to different subregions of posterior parietal cortex.

Cerebellar Input to AIP

To date, we have examined the organization of cerebellar projections to regions of M1, several premotor areas, three areas of dorsolateral prefrontal cortex, a portion of the frontal eye field and a subregion within area 7b (Lynch *et al.*, 1994; Middleton and Strick, 1994, 1996, 1997, 2000, 2001; Hoover and Strick, 1999; Clower *et al.*, 2001a,b; Dum *et al.*, 2002; Dum and Strick, 2003). These cortical areas each receive input from a focal cluster of dentate neurons that we termed an 'output channel' (for references and review, see Dum *et al.*, 2002; Dum and Strick, 2003). In all of our prior studies, we found that the output channels projecting to different cortical areas originate from topographically separate regions of the dentate.

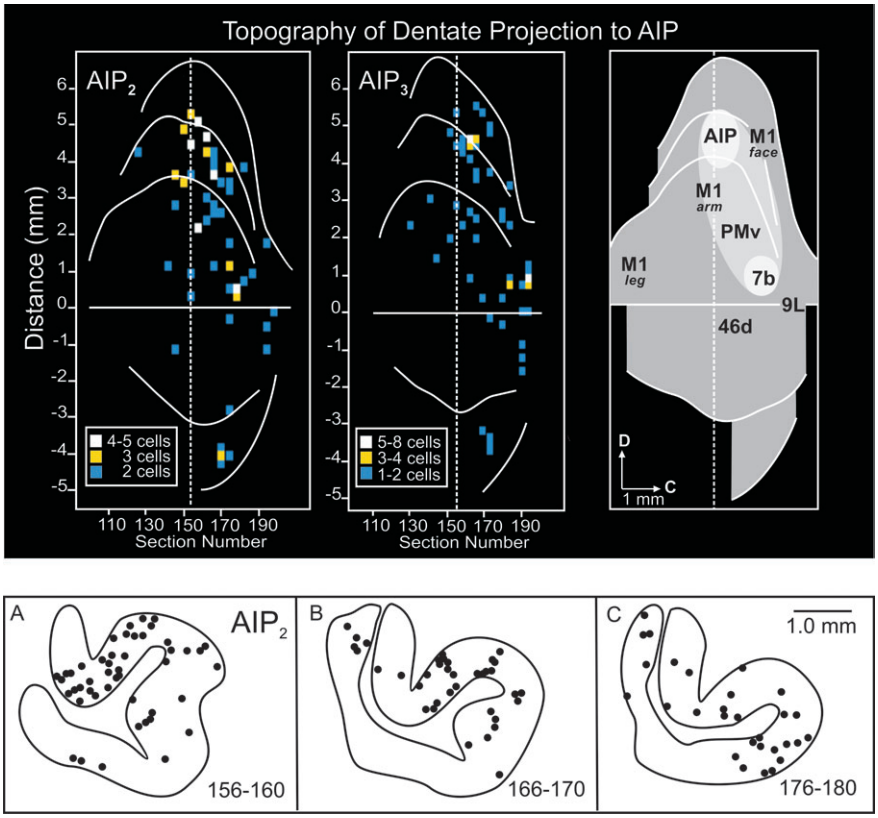

Figure 4. Distribution and density of dentate neurons that project to AIP. Top: unfolded map of the dentate nucleus of AIP_2 (left), AIP_3 (middle), and composite map (right). The maps of the dentate were created by unfolding serial coronal sections through the nucleus (for detailed methods, see Dum and Strick, 2003). The map was reconstructed from every other coronal section through the nucleus. White regions on the composite map indicate areas of densest labeling. The light gray region indicates the location of the low-density field of labeled neurons (see text for details). The labels on the composite map indicate the location of dentate output channels to other frontal, motor and parietal areas of cortex. Bottom: cross sections of the dentate nucleus showing the location of 'second-order' neurons (dots) labeled after transport of rabies virus from AIP. Each panel includes the labeled neurons from three sections (100 μm apart).

Table 1
Subcortical labeling after area AIP injections

Experiment	DN	GPi	SNpr	C:BG
AIP_1 (DC1)	202	64	222	0.7:1
AIP_2 (DC4)	526	48	490	1.0:1
AIP_3 (DC6)	172	24	180	0.8:1

Table 2
Comparison with other cortical regions

Experiment	DN	GPi	SNpr	C:BG
Area AIP (mean, $n = 3$)	300	45	297	0.9:1
PMv (mean, $n = 3$)	682	716	–	1.0:1
M1 arm (mean, $n = 3$)	443	419	–	1.1:1
M1 face (Jo18)	348	652	42	0.5:1
Area 46 (mean, $n = 3$)	218	385	243	0.4:1
Area 12 (mean, $n = 2$)	3	7	309	0.01:1
Area 7b-Sulc (W21)	117	–	44	2.7:1

The results of the present study indicate that the 'output channel' concept does not fully characterize the pattern of cerebellar projections to AIP. AIP is unique in receiving a *broadly distributed*, as well as a focal projection from the dentate. The focal projection originates from a small cluster of dentate neurons that is located dorsally in the dentate at mid rostro-caudal levels. This cluster forms an output channel (via the thalamus) to AIP that is spatially separate from those that project to other cortical areas. AIP also receives input from dentate neurons that are broadly distributed within the nucleus. These neurons are located in dentate regions that also contain output channels to M1, the PMv and perhaps other premotor areas (Dum and Strick, 1999, 2003; Akkal *et al.*, 2001). The local density within this field of labeled neurons is low. However, the entire labeled region contains a substantial component (two-thirds to three-quarters) of the dentate neurons that project to AIP.

Overall, our results indicate that AIP is the target of two patterns of input from the dentate– a small output channel and a broadly distributed field of neurons. This creates a situation in which AIP may receive a sample of the dentate output that is streaming to motor areas in the frontal lobe and may integrate this information with that from its own output channel (Fig. 5, left). The results from other anatomical and physiological studies are consistent with this interpretation (Sasaki *et al.*, 1976; Kakei and Shinoda, 1990; Wannier *et al.*, 1992; Kakei *et al.*, 1995). Thus, some of the complex sensorimotor properties of AIP neurons (Godschalk and Lemon, 1989; Taira *et al.*, 1990; Sakata and Taira, 1994; Sakata *et al.*, 1995, 1998; Murata *et al.*, 1996, 2000) may result from the integration of these inputs. For example, neurons in AIP and PMv have similar neural response patterns during visually guided hand manipulation tasks, and many neurons in both areas show selectivity for both the visual presentation of 3-D objects, as well as the appropriate hand movement for manipulation of a presented object (Murata *et al.*,

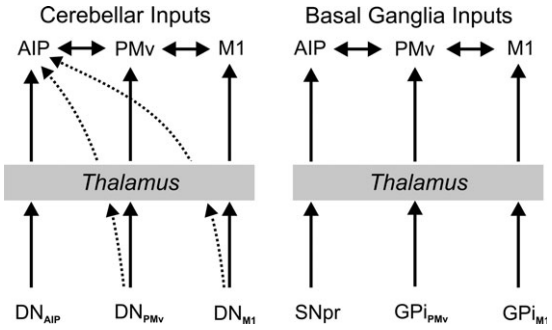

Figure 5. Summary of cerebellar and basal ganglia projections to AIP, PMv and M1. Heavy arrows indicate primary projections from subcortical sites. Dotted arrows indicate a less dense but significant projection. Note that AIP is unique in receiving projections from cerebellar output channels that are mainly directed at other cortical areas.

1997, 2000). Imaging studies during object manipulation have found activation of regions of the human premotor and parietal cortex that may be analogous to the monkey PMv and AIP (Binkofski *et al.*, 1999; Jancke *et al.*, 2001; Mecklinger *et al.*, 2002; Stoeckel *et al.*, 2003). These and other findings have led to the proposal that PMv and AIP together provide a neural substrate for translating the visual properties of a 3-dimensional object into the appropriate hand movement to manipulate that object. The current results add an additional layer of complexity to this picture by demonstrating that AIP, like PMv receives disynaptic input from cerebellum (as well as from the basal ganglia). The cerebellum is thought to be necessary for the adaptive adjustment of motor output and sensorimotor coordination. These mechanisms could have great utility for adjusting hand shape during object manipulation.

Nigral Input to AIP

Retrograde transneuronal transport of rabies virus from AIP injections demonstrated that AIP is a target of output from the basal ganglia. Specifically, we found that AIP receives a projection (via the thalamus) from neurons located in the caudal two-thirds of SNpr. This portion of SNpr also contains some neurons that project to regions of prefrontal cortex (Middleton and Strick, 2002). Because of the complex topography within SNpr, it is difficult to determine whether nigral neurons that project to AIP are segregated from or intermingled with those that project to regions of prefrontal cortex. On the other hand, it is clear that the basal ganglia neurons that project to AIP are entirely segregated from those that project to the cortical motor areas. The cortical motor areas receive basal ganglia input largely from the internal segment of the globus pallidus (GPi) (Hoover and Strick, 1993, 1999; Dum and Strick, 1999; Akkal *et al.*, 2001, 2002). Only the face area of M1 receives some input from neurons located at mid-rostrocaudal levels of SNpr (Hoover and Strick, 1999). However, these SNpr neurons are rostral and dorsolateral to those that project to AIP.

AIP is densely interconnected with the PMv at the cortical level. An obvious question is whether they receive subcortical input from the same sources or even from the same output channels. The answer to this question differs for cerebellar and basal ganglia systems. As noted above, the broadly distributed field of dentate neurons that project to AIP overlaps the dentate output channel to the PMv. In contrast, AIP and PMv receive input from non-overlapping regions of the basal ganglia. PMv is the target of output from GPi, whereas AIP is the target of output from SNpr. These observations suggest that AIP is the target of a separate nigral output channel which is likely to convey information that is functionally distinct from that sent to the PMv and other cortical motor areas.

The demonstration of a nigral input (via the thalamus) to a region of posterior parietal cortex is perhaps the most surprising aspect of the current findings. Classically, the basal ganglia have long been known to receive input from multiple cortical areas including from posterior parietal cortex (e.g. Kemp and Powell, 1971). However, the output of the basal ganglia had been thought to influence primarily motor regions of the cerebral cortex. It is now generally accepted that the output of the basal ganglia also targets regions of prefrontal orbitofrontal and cingulate cortex (for references and review, see Alexander *et al.*, 1986; Middleton and Strick, 2002). We have also provided evidence that the output of the basal ganglia projects to regions of inferotemporal cortex (Middleton and Strick, 1996). The current results reveal that the basal ganglia have an even broader sphere of influence than previously thought. Our report is the first demonstration of an anatomical pathway linking basal ganglia output with the parietal lobe in a primate.

The existence of a nigral projection to AIP clearly expands the potential sphere of influence of the basal ganglia. More importantly, this input may provide an explanation for some of the non-motor deficits observed in patients with Parkinson's disease (PD). Although PD is characterized by motor symptoms, many PD patients display deficits that involve aspects of visuomotor and visuospatial integration (Stern *et al.*, 1983; Boller *et al.*, 1984; Richards *et al.*, 1993; Cronin-Golomb and Braun, 1997; Hocherman and Giladi, 1998; Lee *et al.*, 2001a,b). For example, some PD patients show difficulty on tasks requiring them to mentally rotate a figure before copying it (de Jong *et al.*, 1999). PD patients can also display deficits in making accurate assessments of vertical and horizontal, even when these judgements are reported verbally rather than manually (Danta and Hilton, 1975; Trick *et al.*, 1994; Finton *et al.*, 1998; Montse *et al.*, 2001). These deficits are normally ascribed to dysfunction of posterior parietal cortex. The presence of a disynaptic projection from the nigra to a region of posterior parietal cortex provides an anatomical route to explain these otherwise paradoxical findings.

Notes

We thank M. Page for the development of computer programs and M. O'Malley and C. Lovell for their expert technical assistance. We also thank Drs C. Rupprecht (CDC, Atlanta, GA) for supplying the CVS-11 strain of rabies and A. Wandeler (Animal Diseases Research Institute, Nepean, Ontario, Canada) for supplying antibodies to rabies. This work was supported by the Veterans Affairs Medical Research Service and by US Public Health Service grants NS24328 (P.L.S.) and MH56661 (P.L.S.).

Address correspondence to Dr Peter L. Strick, Department of Neurobiology, University of Pittsburgh School of Medicine, W1640 Biomedical Science Tower, 200 Lothrop Street, Pittsburgh, PA 15261, USA. Email: strickp@pitt.edu

References

Akkal D, Dum RP, Strick PL (2001) Cerebellar and pallidal inputs to the supplementary motor area (SMA). Soc Neurosci Abstr 27:825.4.

Akkal D, Dum RP, Strick PL (2002) Cerebellar and basal ganglia inputs to the pre-supplementary motor area (Pre-SMA). Soc Neurosci Abstr 28:462.14.

Alexander GE, DeLong MR, Strick PL (1986) Parallel organization of functionally segregated circuits linking basal ganglia and cortex. Annu Rev Neurosci 9:357–381.
Barrett AM, Crucian GP, Schwartz R, Nallamshetty H, Heilman KM (2001) Seeing trees but not the forest: limited perception of large configurations in PD. Neurology 56:724–729.
Binkofski F, Buccino G, Stephan KM, Rizzolatti G, Seitz RJ, Freund HJ (1999) A parieto-premotor network for object manipulation: evidence from neuroimaging. Exp Brain Res 128:210–213.
Boller F, Passafiume D, Keefe NC, Rogers K, Morrow L, Kim Y (1984) Visuospatial impairment in Parkinson's disease. Role of perceptual and motor factors. Arch Neurol 41:485–490.
Chavis DA, Pandya DN (1976) Further observations on corticofrontal connections in the rhesus monkey. Brain Res 117:369–386.
Clower DM, West RA, Lynch JC, Strick PL (2001a) The inferior parietal lobule is the target of output from the superior colliculus, hippocampus, and cerebellum. J Neurosci 21:6283–6291.
Clower DM, Dum RP, Strick PL (2001b) Area 7B of parietal cortex is the target of topographical output from the dentate nucleus of the cerebellum. Soc Neurosci Abstr 27:65.9.
Clower DM, Dum RP, Strick PL (2002) Substantia nigra pars reticulata provides input to area 7B of parietal cortex. Soc Neurosci Abstr 28:460.1.
Cronin-Golomb A, Braun AE (1997) Visuospatial dysfunction and problem solving in Parkinson's disease. Neuropsychology 11:44–52.
Danta G, Hilton RC (1975) Judgment of the visual vertical and horizontal in patients with Parkinsonism. Neurology 25:43–47.
de Jong BM, Frackowiak RS, Willemsen AT, Paans AM (1999) The distribution of cerebral activity related to visuomotor coordination indicating perceptual and executional specialization. Brain Res Cogn Brain Res 8:45–59.
Dum RP, Strick PL (1991) The origin of corticospinal projections from the premotor areas in the frontal lobe. J Neurosci 11:667–689.
Dum RP, Strick PL (1999) Pallidal and cerebellar inputs to the digit representations of the dorsal and ventral premotor areas (PMd and PMv). Soc Neurosci Abstr 25:1925.
Dum RP, Strick PL (2002) Motor areas in the frontal lobe of the primate. Physiol Behav 77:677–682.
Dum RP, Strick PL (2003) An unfolded map of the cerebellar dentate nucleus and its projections to the cerebral cortex. J Neurophysiol 89:634–639.
Dum RP, Li C, Strick PL (2002) Motor and nonmotor domains in the monkey dentate. Ann N Y Acad Sci 978:289–301.
Finton MJ, Lucas JA, Graff-Radford NR, Uitti RJ (1998) Analysis of visuospatial errors in patients with Alzheimer's disease or Parkinson's disease. J Clin Exp Neuropsychol 20:186–193.
Francois C, Percheron G, Yelnik J (1984) Localization of nigrostriatal, nigrothalamic and nigrotectal neurons in ventricular coordinates in macaques. Neuroscience 13:61–76.
Ghosh S, Gattera R (1995) A comparison of the ipsilateral cortical projections to the dorsal and ventral subdivisions of the macaque premotor cortex. Somatosens Mot Res 12:359–378.
Godschalk M, Lemon RN (1989) Preparation of visually cued arm movements in monkey. Involvement of inferior parietal cortex. Brain Behav Evol 33:122–126.
Godschalk M, Lemon RN, Kuypers HG, Ronday HK (1984) Cortical afferents and efferents of monkey postarcuate area: an anatomical and electrophysiological study. Exp Brain Res 56:410–424.
He SQ, Dum RP, Strick PL (1993) Topographic organization of corticospinal projections from the frontal lobe: motor areas on the lateral surface of the hemisphere. J Neurosci 13:952–980.
He SQ, Dum RP, Strick PL (1995) Topographic organization of corticospinal projections from the frontal lobe: motor areas on the medial surface of the hemisphere. J Neurosci 15:3284–3306.
Hocherman S, Giladi N (1998) Visuomotor control abnormalities in patients with unilateral parkinsonism. Neurology 50:1648–1654.
Holsapple JW, Preston JB, Strick PL (1991) The origin of thalamic inputs to the 'hand' representation in the primary motor cortex. J Neurosci 11:2644–2654.
Hoover JE, Strick PL (1993) Multiple output channels in the basal ganglia. Science 259:819–821.
Hoover JE, Strick PL (1999) The organization of cerebellar and basal ganglia outputs to primary motor cortex as revealed by retrograde transneuronal transport of herpes simplex virus type 1. J Neurosci 19:1446–1463.
Jancke L, Kleinschmidt A, Mirzazade S, Shah NJ, Freund HJ (2001) The role of the inferior parietal cortex in linking the tactile perception and manual construction of object shapes. Cereb Cortex 11: 114–121.
Kakei S, Shinoda Y (1990) Parietal projection of thalamocortical fibers from the ventroanterior-ventrolateral complex of the cat thalamus. Neurosci Lett 117:280–284.
Kakei S, Yagi J, Wannier T, Na J, Shinoda Y (1995) Cerebellar and cerebral inputs to corticocortical and corticofugal neurons in areas 5 and 7 in the cat. J Neurophysiol 74:400–412.
Kelly RM and Strick PL (2000) Rabies as a transneuronal tracer of circuits in the central nervous system. J Neurosci Methods 103: 63–71.
Kelly RM, Strick PL (2003) Cerebellar loops with motor cortex and prefrontal cortex of a nonhuman primate. J Neurosci 23: 8432–8444.
Kemp JM, Powell TP (1971) The connexions of the striatum and globus pallidus:synthesis and speculation. Philos Trans R Soc Lond B Biol Sci 262:441–457.
Langer LF, Graybiel AM (1989) Distinct nigrostriatal projection systems innervate striosomes and matrix in the primate striatum. Brain Res 498:344–350.
Lee AC, Harris JP, Atkinson EA, Fowler MS (2001a) Evidence from a line bisection task for visuospatial neglect in left hemiparkinson's disease. Vision Res 41:2677–2686.
Lee AC, Harris JP, Atkinson EA, Fowler MS (2001b) Disruption of estimation of body-scaled aperture width in Hemiparkinson's disease. Neuropsychologia 39:1097–1104.
Lewis JW, Van Essen DC (2000) Corticocortical connections of visual, sensorimotor, and multimodal processing areas in the parietal lobe of the macaque monkey. J Comp Neurol 428:112–137.
Luppino G, Murata A, Govoni P, Matelli M (1999) Largely segregated parietofrontal connections linking rostral intraparietal cortex (areas AIP and VIP) and the ventral premotor cortex (areas F5 and F4). Exp Brain Res 128:181–187.
Lynch JC, Hoover JE, Strick PL (1994) Input to the primate frontal eye field from the substantia nigra, superior colliculus, and dentate nucleus demonstrated by transneuronal transport. Exp Brain Res 100:181–186.
Matelli M, Camarda R, Glickstein M, Rizzolatti G (1984) Interconnections within the postarcuate cortex (area 6) of the macaque monkey. Brain Res 310:388–392.
Matelli M, Camarda R, Glickstein M, Rizzolatti G (1986) Afferent and efferent projections of the inferior area 6 in the macaque monkey. J Comp Neurol 251:281–298.
Mecklinger A, Gruenewald C, Besson M, Magnie MN, Von Cramon DY (2002) Separable neuronal circuitries for manipulable and non-manipulable objects in working memory. Cereb Cortex 12:1115–1123.
Mesulam MM (1982) Tracing neural connections. New York: Wiley.
Middleton FA, Strick PL (1994) Anatomical evidence for cerebellar and basal ganglia involvement in higher cognitive function. Science 266:458–461.
Middleton FA, Strick PL (1996) The temporal lobe is a target of output from the basal ganglia. Proc Natl Acad Sci USA 93:8683–8687.
Middleton FA, Strick PL (1997) Cerebellar output channels. Int Rev Neurobiol 41:61–82.
Middleton FA, Strick PL (2000) Basal ganglia and cerebellar loops:motor and cognitive circuits. Brain Res Brain Res Rev 31:236–250.
Middleton FA, Strick PL (2001) Cerebellar projections to the prefrontal cortex of the primate. J Neurosci 21:700–712.
Middleton FA, Strick PL (2002) Basal-ganglia 'projections' to the prefrontal cortex of the primate. Cereb Cortex 12:926–935.
Montse A, Pere V, Carme J, Francesc V, Eduardo T (2001) Visuospatial deficits in Parkinson's disease assessed by judgment of line orientation test:error analyses and practice effects. J Clin Exp Neuropsychol 23:592–598.

Murata A, Gallese V, Kaseda M, Sakata H (1996) Parietal neurons related to memory-guided hand manipulation. J Neurophysiol 75:2180–2186.
Murata A, Fadiga L, Fogassi L, Gallese V, Raos V, Rizzolatti G (1997) Object representation in the ventral premotor cortex (area F5) of the monkey. J Neurophysiol 78:2226–2230.
Murata A, Gallese V, Luppino G, Kaseda M, Sakata H (2000) Selectivity for the shape, size, and orientation of objects for grasping in neurons of monkey parietal area AIP. J Neurophysiol 83:2580–2601.
Neal JW, Pearson RC, Powell TP (1990) The ipsilateral cortico-cortical connections of area 7b, PF, in the parietal and temporal lobes of the monkey. Brain Res 524:119–132.
Oztop E, Arbib MA (2002) Schema design and implementation of the grasp-related mirror neuron system. Biol Cybern 87:116–140.
Percheron G, Francois C, Talbi B, Yelnek J, Fenelon G (1996) The primate motor thalamus. Brain Res Rev 22:93–181.
Petrides M, Pandya DN (1984) Projections to the frontal cortex from the posterior parietal region in the rhesus monkey. J Comp Neurol 228:105–116.
Preuss TM, Goldman-Rakic PS (1991) Architectonics of the parietal and temporal association cortex in the strepsirhine primate *Galago* compared to the anthropoid primate *Macaca*. J Comp Neurol 310: 475–506.
Richards M, Cote LJ, Stern Y (1993) The relationship between visuospatial ability and perceptual motor function in Parkinson's disease. J Neurol Neurosurg Psychiatry 56:400–406.
Rosene DL, Mesulam MM (1978) Fixation variables in horseradish peroxidase neurohistochemistry. I. The effect of fixation time and perfusion procedures upon enzyme activity. J Histochem Cytochem 26:28–39.
Rosene DL, Roy N, Davis BJ (1986) A cryoprotection method that facilitates cutting frozen sections of whole monkey brains for histological and histochemical processing without freezing artifact. J Histochem Cytochem 34:1301–1315.
Sakata H, Taira M (1994) Parietal control of hand action. Curr Opin Neurobiol 4:847–856.
Sakata H, Taira M, Murata A, Mine S (1995) Neural mechanisms of visual guidance of hand action in the parietal cortex of the monkey. Cereb Cortex 5:429–438.
Sakata H, Taira M, Kusunoki M, Murata A, Tanaka Y (1997) The TINS Lecture. The parietal association cortex in depth perception and visual control of hand action. Trends Neurosci 20: 350–357.
Sakata H, Taira M, Kusunoki M, Murata A, Tanaka Y, Tsutsui K (1998) Neural coding of 3D features of objects for hand action in the parietal cortex of the monkey. Philos Trans R Soc Lond B Biol Sci 353: 1363–1373.
Sasaki K, Kawaguchi S, Oka H, Sakai M, Mizuno N (1976) Electrophysiological studies on the cerebellocerebral projections in monkeys. Exp Brain Res 24:495–507.
Stern Y, Mayeux R, Rosen J, Ilson J (1983) Perceptual motor dysfunction in Parkinson's disease: a deficit in sequential and predictive voluntary movement. J Neurol Neurosurg Psychiatry 46:145–151.
Stoeckel MC, Weder B, Binkofski F, Buccino G, Shah NJ, Seitz RJ (2003) A fronto-parietal circuit for tactile object discrimination:an event-related fMRI study. Neuroimage 19:1103–1114.
Strick PL, Card JP (1992) Transneuronal mapping of neural circuits with alpha herpesviruses. In: Experimental neuroanatomy: a practical approach (Bolam JP, ed.), pp. 81–101. Oxford: Oxford University Press.
Strick PL, Preston JB (1982a) Two representations of the hand in area 4 of a primate. II. Somatosensory input organization. J Neurophysiol 48:150–159.
Strick PL, Preston JB (1982b) Two representations of the hand in area 4 of a primate. I. Motor output organization. J Neurophysiol 48:139–149.
Suzuki H, Azuma M (1976) A glass-insulated 'Elgiloy' microelectrode for recording unit activity in chronic monkey experiments. Electroencephalogr Clin Neurophysiol 41:93–95.
Taira M, Mine S, Georgopoulos AP, Murata A, Sakata H (1990) Parietal cortex neurons of the monkey related to the visual guidance of hand movement. Exp Brain Res 83:29–36.
Tanne-Gariepy J, Rouiller EM, Boussaoud D (2002) Parietal inputs to dorsal versus ventral premotor areas in the macaque monkey: evidence for largely segregated visuomotor pathways. Exp Brain Res 145:91–103.
Trick GL, Kaskie B, Steinman SB (1994) Visual impairment in Parkinson's disease: deficits in orientation and motion discrimination. Optom Vis Sci 71:242–245.
Wannier T, Kakei S, Shinoda Y (1992) Two modes of cerebellar input to the parietal cortex in the cat. Exp Brain Res 90:241–252.
Williams SM, Goldman-Rakic PS (1998) Widespread origin of the primate mesofrontal dopamine system. Cereb Cortex 8:321–345.